GEOLOGICA CARPATHICA, AUGUST 2010, 61, 4, 257–272 doi: 10.2478/v10096-010-0015-2

Stratigraphic correlation potential of magnetic susceptibility and gamma-ray spectrometric variations in calciturbiditic facies (Silurian-Devonian boundary, Prague Synclinorium, Czech Republic)

FRANTIŠEK VACEK[1], JINDŘICH HLADIL[2] and PETR SCHNABL[2]

[1]Charles University in Prague, Faculty of Science, Institute of Geology and Palaeontology, Albertov 6, 128 43 Prague 2, Czech Republic; fvacek@natur.cuni.cz
[2]Institute of Geology AS CR, v.v.i., Rozvojová 269, 165 00 Prague 6, Czech Republic; hladil@gli.cas.cz

(Manuscript received November 9, 2009; accepted in revised form March 11, 2010)

Abstract: Magnetic susceptibility (MS) and gamma-ray spectrometry (GRS) stratigraphy were used for correlation and characterization of eight Silurian-Devonian (S-D) sections in the Prague Synclinorium (Czech Republic). They represent two different facies developments: lower subtidal to upper slope deposits and slope-to-basin-floor distal calciturbidites. Sections from relatively shallow- and deep-water sections are easy to compare and correlate separately, although the detailed relationship between these two facies is still not entirely clear and correlations between the two settings are difficult. This may be due to sharp facies transitions and presence of stratigraphic gaps. The MS and GRS stratigraphic variations combined with sedimentologic data have been also used for reconstruction of the evolution of the sedimentary environment. The beds close above the S-D boundary show noticeably enhanced MS magnitudes but weak natural gamma-ray emissions. It may correspond to an increased amount of terrigenous magnetic material occurring with short-term shallowing (sedimentological evidence). In deep-water sections the uppermost Silurian is characterized by high MS and GRS values. It corresponds to a supply of recycled sediment to the lower wedge which occurred during the late Pridoli regression phase. The basal Devonian beds correspond to gradual deepening, but the overlying sequences reflect other shallowing episodes which are expressed in increasing MS and gamma ray activity of rocks. The MS and GRS fluctuations are interpreted as a result of local subsidence of the sea bottom along synsedimentary growth-faults and/or a biotic event rather than of eustatic sea-level changes.

Key words: Silurian-Devonian boundary, Prague Synclinorium, magnetic susceptibility stratigraphy, gamma-ray spectrometry, carbonate slope system.

Introduction

The Prague Synclinorium in central Bohemia (Czech Republic) provides many instructive sections exposing the Silurian-Devonian (Pridoli-Lochkovian) boundary strata, including the Global Boundary Stratotype Section and Point (GSSP) Klonk near Suchomasty and its auxiliary section at Budňanská skála (Budňany Rock) near Karlštejn. Two standard sections were approved by a decision of the International Commission on Stratigraphy at the 24th International Geological Congress in Montreal, 1972 (McLaren 1977). During more than thirty years of investigation these standard sections have been studied by various methods. Stratigraphic correlations here were traditionally based mainly on biostratigraphic data. In this stratigraphic succession graptolites and trilobites are practical for biozonation. However, the occurrences of index species depend on facies to various degrees. Microfossils, namely conodonts and Chitinozoa have high resolution potential, but detailed micropaleontological research was predominantly concentrated on the standard sections (Paris et al. 1981; Jeppsson 1988, 1989; Brocke et al. 2002, 2006; Carls et al. 2007). In many other sections precise biostratigraphic data are incomplete to mostly absent. In several recent papers different stratigraphic approaches were applied, including magnetic susceptibility (MS) stratigraphy (Crick et al. 2001) or chemostratigraphy (Hladíková et al. 1997; Herten 2000; Kranendonck 2000; Mann et al. 2001; Frýda et al. 2002; Buggisch & Mann 2004). Crick et al. (2001) introduced the MS stratigraphic profile for the GSSP at Klonk and a drilling core situated close to the surface section. They used the MS record for establishment of magnetosusceptibility event and cyclostratigraphic (MSEC) zones as an alternative stratigraphic tool. They also suggested possible interregional correlations with the area of the Anti-Atlas in Morocco using MSEC.

This study involves eight sections, which have been studied before for paleontology and sedimentology, but not for MS and GRS (gamma-ray spectrometry) stratigraphic variations. Both methods will be tested for the detailed stratigraphic correlations across varying facies and could also be used in combination with supplementary data for complex characteristics of the depositional environment and its evolution in several Silurian-Devonian (S-D) boundary sections in the Prague Synclinorium.

Geological setting

The Variscan folded Silurian and Devonian formations crop out in the central part of the Prague Synclinorium between Prague and vicinity of Beroun (Fig. 1). They consist of marine sediments (mostly shales and limestones; Chlupáč et al. 1998) and submarine volcanic rocks (basic volcanics and coeval basic/ultrabasic volcaniclastics; Fiala 1970; Patočka & Štorch 2004). Prague Synclinorium was interpreted as located on the northern margins of Gondwana during the S-D interval with affinities to Armorica (e.g. Krs & Pruner 1995; Krs et al. 2001), at a paleolatitude of about 17°S (Patočka et al. 2003).

The S-D boundary is situated close to the boundary between the Požáry (approximately corresponding to the Pridoli Series) and Lochkov Formations (~the Lochkovian Stage). Both formations are generally characterized by lateral transition from coarse-grained bioclastic limestones in the NW part of the synclinorium to fine-grained limestones and shales in the SE part (Chlupáč et al. 1998), defining a NW shallow zone and SE deeper zone. However, the boundaries of these two lithostratigraphic units are slightly diachronous over the region. Proximity of the S-D boundary is broadly characterized by blooms of pelagic crinoids with plate-type loboliths, typically *Scyphocrinites*, which often (but not always) occur in the beds of the latest Pridoli and early Lochkovian ages. They may form several meters thick beds of coarse-grained crinoidal limestones at the base of the Lochkov Formation, informally called the *Scyphocrinites* Horizon (*Scyphocrinites* H). It may be locally associated with cephalopod limestones and also with beds of flat-pebble conglomerates. It is better recognizable in the deeper zone because in the shallow-water environment it may be concealed by overall bioclastic deposition.

Several localities exposing the S-D boundary strata representing the two different facies were selected for study (see Fig. 1, Table 1). These facies were deposited on the margin of an open-sea carbonate shelf with adjacent carbonate slope environment (Vacek 2007). Generally a deepening trend can be traced from the NW to the SE of the basin.

Methods

Limestone "beds" are traditionally numbered 1, 2, 3, etc., designations such as 1/2, 2/3 are used for the shale "interbeds".

Magnetic susceptibility study

In the last ten years, the number of studies on stratigraphic MS variations in the Devonian marine carbonate or mixed sequences has increased significantly (Crick et al. 1997, 2000, 2001, 2002; Ellwood et al. 2000, 2001, 2006; da Silva & Boulvain 2006; Hladil et al. 2006; da Silva et al. 2009a,b, 2010; Koptíková et al. 2010).

The outcrop sections were sampled for the MS study at 0.05 m intervals. Small cubic or slice rock samples were collected (20–50 g). Only fresh samples were taken (i.e. avoiding the veins, visible pyrite or limonite aggregates, various spots related to late diagenetic alterations and weathering, epigenetic dolomitization and also shear-deformed parts of the rock). The thickness of the MS profiles ranges from 4 to 11 meters depending on geological conditions. The complete sample collection includes more than 1,000 samples. Measurements were carried out in the Laboratory of Paleomagnetism (Inst. Geol. AS CR, Prague) on Kappabridges KLY-2 and 3 (produced by Agico Ltd. Brno; for technical details we refer to www.agico.com). The values of magnetic susceptibility in this paper are expressed as mass-related magnetic susceptibility (10^{-9} $m^3 \cdot kg^{-1}$). These are further referred as MS values which are used for plotting the curves and assessment of their possible stratigraphic importance.

Magnetic susceptibility is the intrinsic property that determines the amount of magnetism, which a rock can have in a given magnetic field. It is related to bulk chemistry and magnetic mineralogy and particularly to the amounts of easily magnetizable minerals in a rock sample. The increased MS signal in limestones is induced by presence of various ferromagnetic (s.l.) minerals (magnetite, maghemite, hematite, monoclinic pyrrhotite), and also weakly magnetic but much more abundant paramagnetic minerals (clay minerals, pyroxene, amphibole, biotite, chlorite, pyrite, chalcopyrite, a.o.).

In contrast, diamagnetic minerals such as calcite, quartz, and others have very weak negative MS magnitudes and reduce mass susceptibility of a rock sample. However, the MS of detrital ferromagnetic and paramagnetic minerals is much greater than the MS of diamagnetic minerals. Therefore, a small amount of even weakly paramagnetic mineral can significantly outweigh the MS of volumetrically more abundant diamagnetic minerals (Ellwood et al. 2000).

The amount of magnetic particles mainly depends on terrigenous influx, which is mostly controlled by fluctuations in sea level. Generally, the maximum input of terrigenous detritus corresponds to intensive erosion during the lowstand of sea level. This is considered to be recognizable on both the regional and global scale because of synchronous variations in global erosion controlled by eustasy (Ellwood et al. 2000, 2001). The large-scale redistribution of sub-silt and silt-sized particles (< 63 μm) often comes about through eolian transport, and the deep parts of carbonate slopes can also be affected by distant riverine flux (Hladil 2002; Hladil et al. 2006).

Magnetite can also be produced by magnetotactic bacteria or algae. However, it is mostly formed in shallow-water conditions with restricted circulation, which is not the case of the studied sections. The other magnetically important mineral components related to deep-water carbonate or mixed carbonate-siliciclastic sediments are authigenic carbonates with iron in lattices or iron-oxide inclusions (siderite and rarely other minerals; e.g. Ellwood et al. 1988; Frederichs et al. 2003), and these are also tentatively related to bacterially-mediated precipitates. For more discussion on the primary and secondary magnetic minerals in carbonates we refer to da Silva et al. (2009a).

Rock magnetic methods

Several methods have been used for identification of possible carriers of the MS. They have been applied both on miner-

al concentrates obtained by dissolution in acids (10 samples; X-ray diffraction — XRD; temperature dependence of the MS; magnetic hysteresis) and the whole-rock samples (5 samples; isothermal remanent magnetization — IRM).

Mineral concentrates have been obtained by leaching in 10% hydrochloric and acetic acids, separately. However, some important magnetic minerals such as iron oxides may be dissolved in these acids, therefore we had to also use the IRM method applied to whole rock (see above).

The method of temperature dependent MS identifies magnetic minerals and mineralogical phase changes during heating. It was measured using KLY-4S Kappabridge (produced by Agico Ltd. Brno; Jelínek & Pokorný 1997) combined with a temperature control unit CS3 (Parma & Zapletal 1991) in the temperature range of 20–700 °C in an argon atmosphere. Paramagnetic minerals exhibit parabolic-shaped MS decay curves at relatively low temperatures (up to ~200 °C) because the MS of these minerals is inversely proportional to the temperature (Hrouda 1994). On the other hand, ferromagnetic minerals usually show increasing MS up to the point where it decays to the Curie temperature. For magnetite the Curie temperature is ~580 °C and for hematite it is ~680 °C.

The method of magnetic hysteresis is based on response of a magnetic material to magnetic field. Hysteretic behaviour is highly dependent on mineralogy and grain size (Tauxe et al. 1996). The sample is placed in an intensive magnetic field (+1 T) and magnetization is examined as the applied intensity drops to zero and then increases to the negative maximum (–1 T). Changes in magnetization during regaining of the original intensity (+1 T) are significant for interpretation of magnetic components. These measurements were performed on a vibrating sample magnetometer Model 3900 VSM (produced by Princeton Measurement Corporation).

IRM was measured on Pulse Magnetizer MMPM 10 (produced by Magnetic Measurements Ltd.) and magnetometer JR6a (produced by Agico Ltd. Brno) in order to identify coercivity spectra. The used field range was 10 to 2000 mT. Contribution of particular magnetic components ferromagnetic to the total remanent magnetization has been tested by the IRM component analysis (Kruiver et al. 2001). Various magnetic minerals can be identified by $B_{1/2}$ values, which is the magnetic field at which a half of Saturated Isothermal Remanent Magnetization (SIRM) is reached. For magnetite it is 20–63 mT, hematite 63–200 mT, and goethite >1 T (Grygar et al. 2003).

Gamma ray spectrometry study

The spectral gamma-ray approach is a significant parallel to MS-detected concentrations of background sediment impurity in limestone (Hladil et al. 2006). The MS-GRS combination has an overall potential to improve the quality of MS based stratigraphic correlation, with the background reasoning in magnetomineralogy.

The gamma-ray spectrometric (GRS) based correlations of outcrop logs have been frequently used in the last decade in the Devonian of the Czech Republic on the platform to basin formations of Moravia (Hladil et al. 2000, 2003a,b; Hladil 2002; Geršl & Hladil 2004; Bábek et al. 2007, a.o.) or Prague Synclinorium (Slavík et al. 2000; Koptíková et al. 2007, 2008, 2010).

For this study, a gamma-ray spectrometer Geofyzika-Satis-Geo GS-512 with NaI(Tl) scintillation detector 3″×3″ (7.62×7.62 cm) and 3″ photomultiplier was used (SatisGeo 2009). This instrument was used in the mode that the whole element concentrations of K (%), U (mg/kg=ppm) and Th (ppm) were automatically calculated. The instrument was calibrated at the regional reference centre of Bratkovice near Příbram (parameters frequently quoted, e.g. Lis et al. 1997). Using this technique and instrument, the gamma rays registered for this purpose correspond to isotopes ^{214}Bi and ^{208}Tl, uranium and thorium decay series isotopes in naturally occurring materials, respectively. The data on potassium is obtained using the spectra for ^{40}K isotope. The total natural gamma-ray variation has been inferred from selected energy windows, all above 720 keV. With this instrument, this additional parameter is set to display automatically a notional uranium equivalent (eU) that is routinely expressed in mg/kg (ppm) of U-equivalent contents, but for imagination or rough comparison only. In addition, the recalculation to API units or radioactive doses cannot be accomplished in general terms, for its relationships to techniques, conditions and details of probes or instruments (Geršl & Hladil 2004). These approximate data on the totals of natural gamma ray (NGR or GR) emission from measured sedimentary rocks often differs according to apparatuses and has, therefore, only relative and not absolute information value.

The thicknesses of the GRS logs are identical with the MS ones, except the lower part of the Praha-Podolí section, which could not be measured due to its intensive weathering.

The GRS measurement was performed with 0.25 m step at a time of 240 seconds, perpendicular to the rock face at the full contact. This regular spacing strategy was preferred over the irregular (rock-type selective) one. This choice was based on the preliminary-test findings that gamma-ray signal of different magnitudes and structure was obtained from the beds of comparable lithology (e.g. great variation within the class of coarse-grain calciturbidites, or the same for the very fine-grained shale interbeds). The size of this 0.25 m step was selected heuristically but with respect to the fact that approximately 95% signal at the front of the probe (with crystal) originates from a slightly deformed hemisphere of measured rocks that corresponds to a target of 0.25 m radius at an ideal planar surface (Løvborg et al. 1971). Hence, this empirically tested precondition for overlapping of measurements with these sections makes possible to keep the overlap below 15 % of the signal, even for irregular arrangements of beds and rock materials. The combined error from conditions, instrument and repeated measurements was established to be less than about ±7.5 % for the whole element U, Th, K automatically calculated results.

Detected concentrations of K, U, and Th are mostly related to amount of feldspars, micas, and clay minerals, among others. Uranium is also known to be remarkably trapped in organic matter (e.g. Durrance 1986). Higher concentrations of these elements should again reflect increased amount of non-carbonate impurities in limestones that are caused by detrital

influx from a supposed land surface in both the regional and interregional contexts.

Sedimentology and studied sections

The lithology, sedimentology, and biostratigraphy of the selected sections have been described in many previous papers (for more details we refer to Chlupáč et al. 1972; Hladil 1991, 1992; Čáp et al. 2003; Vacek 2007).

Shallow facies

The relatively shallow-water carbonate facies with predominance of bioclastic, mainly crinoidal packstones to grainstones is distributed in the NW flank of the synclinorium with several other finger-like projections in its western part (studied sections at Požáry Quarry near Praha-Řeporyje, Srbsko, and Opatřilka Quarry near Praha-Holyně; Fig. 1, Table 1). These deposits locally show reworking by storms, which indicates the conditions above the storm wave base. It corresponds to the lower subtidal to upper slope environment.

The shallow-water carbonate facies possess rich benthic fauna, including crinoids and trilobites, and brachiopods. The uppermost Silurian is characterized by abundant occurrence of the index trilobite *Tetinia minuta*. The first appearance of trilobite *Warburgella rugulosa rugosa* indicates the base of Devonian (Chlupáč et al. 1972).

Deep facies

Deep-water facies are distributed in the SE flank of the Prague Synclinorium (sections at Karlštejn, Klonk, Praha-Radotín and Praha-Podolí; Fig. 1, Table 1). These facies are characterized as dark bioclastic and peloidal wackestones/packstones to mudstones alternating with calcareous shales, locally with several meters thick *Scyphocrinites* H. They yield common pelagic fauna, including graptolites, cephalopods and ostracods. The S-D boundary interval is characterized by abundant occurrence of crinoids of *Scyphocrinites* sp. The uppermost Silurian corresponds to the graptolite *Monograptus transgrediens* Zone. The base of Devonian is marked by the first appearance of the index graptolite *Monograptus uniformis* (Chlupáč et al. 1972). Other fossil groups (conodonts,

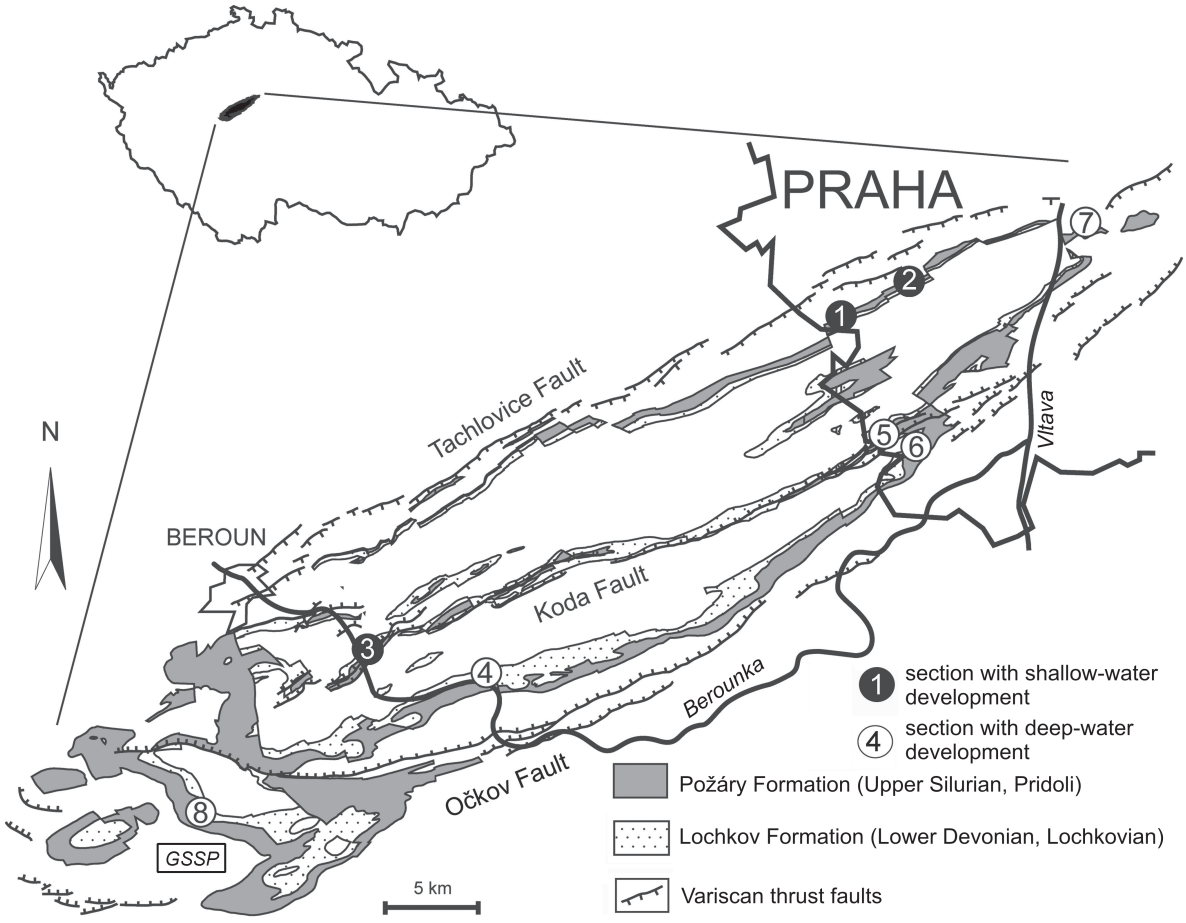

Fig. 1. Position of the studied localities in the Prague Synclinorium area: **1** — Požáry Quarry near Praha-Řeporyje; **2** — Opatřilka Quarry near Praha-Holyně; **3** — Srbsko; **4** — Karlštejn (Budňany Rock); **5** — Praha-Radotín (U topolů); **6** — Praha-Radotín (near Cement Plant); **7** — Praha-Podolí; **8** — Klonk near Suchomasty. **GSSP** — Global Boundary Stratotype Section and Point. The geological sketch map of the Prague Synclinorium benefits partly from the working materials provided by R. Melichar.

Table 1: List of studied sections with their geographical position, measured intervals and numbers of analysed MS samples and GRS measurements. * The GRS measurements were performed in the bed interval 10–12 only due to poor state of the lower part of the section.

No.	Section	Location	Sampling interval	MS	GRS	Environment
1	Požáry Quarry	50° 1' 42.3" N; 14° 19' 28.4" E	beds 155–163 (9 m)	177	36	Shallow
2	Opatřilka Quarry	50° 2' 8.1" N; 14° 21' 2.7" E	beds 1–8 (10 m)	200	41	Shallow
3	Srbsko	49° 56' 29.6" N; 14° 7' 57.2" E	beds 1–3 (6 m)	120	25	Shallow
4	Karlštejn	49° 56' 4.5" N; 14° 10' 51.4" E	beds 1–42 (11 m)	224	45	Deep
5	Praha-Radotín (U topolů)	49° 59' 51.2" N; 14° 20' 2.6" E	beds 1–31 (7 m)	141	28	Deep
6	Praha-Radotín (near Cement Plant)	49° 59' 33.9" N; 14° 20' 46.4" E	beds 9–14 (3.5 m)	70	15	Deep
7	Praha-Podolí	50° 3' 6.9" N; 14° 25' 7.6" E	beds 1–11 (3.5 m)	76	9*	Deep
8	Klonk near Suchomasty	49° 54' 1.3" N; 14° 3' 46.3" E	1–44 (12.75 m)	adopted from Crick et al. (2001)	52	Deep

Chitinozoa) can be used as auxiliary indicators (Paris et al. 1981; Brocke et al. 2002, 2006; Carls et al. 2007).

This facies is interpreted as rhythmical distal calciturbidites deposited on carbonate slope and its toe (often with the Bouma Tc and Td units). These turbidite beds alternate with layers of the "background" hemipelagic sediments (Te), which are preserved mostly in the form of highly compacted calcareous shales. The occurrences of channelized calciturbidite grainstones and rudstones with several layers of flat pebble conglomerates are interpreted as debris flow deposits or dense turbidite flows. The input of the coarse-grained detrital material of shallow-water origin was interpreted as the result of relative sea-level drop in the S-D boundary interval and possible subsidence along synsedimentary growth faults (Vacek 2007).

The MS and GRS stratigraphy of the studied sections

Main characteristics of the MS and GRS records of the shallow facies

Generally, the carbonate rocks in the studied sections have relatively low MS signal in the order of 10^{-9} $m^3 \cdot kg^{-1}$ (further referred as 10^{-9} SI Units). Shallow-water bioclastic packstones/grainstones exhibit relatively low differences of the average MS values between the Požáry and Lochkov Formations (see Table 2, Fig. 2). The MS curves mostly show only low to moderate oscillations (see Fig. 2). The critical S-D boundary interval in the shallow-water deposits (especially the Požáry Q and Opatřilka sections) is marked by enhanced MS values. In the Požáry Q this increase is observable directly above the boundary in the lowermost part of bed No. 159 (see Fig. 2A). In the Opatřilka section, the same pattern characterized by high oscillation is recognizable in bed No. 8 approximately 1 m above the first appearance of *W. rugulosa rugosa*, which determines the S-D boundary (Fig. 2B). However, this pattern is less distinctive in the Srbsko section (Fig. 2C).

This facies is characterized by relatively low concentrations and variations of potassium in the Požáry and Srbsko sections (0.3–0.5 %; Table 2). The concentrations of K show a considerably weak covariance with those of Th (R^2=0.37 and 0.47). On the contrary, at Opatřilka this covariance is very high (R^2=0.91). Correlation between K and U and Th and U is also generally weak, with the concentration of U changing quite independently of K and Th. Trends of the eU curves visually correspond mostly to variations of U, less to Th concentrations (Fig. 2A–C). It corresponds well to the fact that the Th/U ratio is generally very low, with an average of 0.17–0.39 (i.e. the GRS-based concentrations for U are much higher than

Table 2: Average magnitudes of the MS and GRS-based concentrations in the studied sections or their distinguished segments. **S** — Silurian; **D** — Devonian; **Po** — Požáry Fm; **Sc** — *Scyphocrinites* H; **Lo** — Lochkov Fm. The uppermost part of the Požáry Fm in the Podolí section was not GRS measured due to weathering. The "raw" MS data for the Klonk section were not available.

Sections/their segments	MSχ [10^{-9} $m^3 \cdot kg^{-1}$]	eU [ppm]	K [%]	U [ppm]	Th [ppm]
Požáry Q. *Po* (0.0–4.40 m)	9.8	7.5	0.5	5.3	1.5
Lo (4.45–8.7 m)	11.0	5.8	0.5	3.8	1.5
Srbsko *Po* (0.0–4.75 m)	7.3	4.5	0.3	3.6	0.9
Lo (4.8–6.0 m)	5.3	4.6	0.4	2.7	0.8
Opatřilka Q. *Po* (0.0–6.5 m)	9.0	14.9	1.0	10.3	2.1
Lo (6.55–9.9 m)	11.3	11.7	0.3	10.6	1.0
Klonk *Po* (0.0–5.25 m)	–	13.6	1.7	5.2	5.1
Lo (5.3–12.75 m)	–	8.8	1.2	3.1	3.2
Karlštejn *Po* (0.0–2.45 m)	30.2	22.4	1.7	13.6	5.6
Sc (2.5–7.45 m)	1.8	8.4	0.5	6.1	1.6
Lo (7.5–11.1 m)	10.2	7.2	0.8	3.6	2.3
U topolů *Po* (0.0–1.95 m)	28.9	14.8	1.9	6.0	4.6
Sc (2.0–3.35 m)	3.8	13.0	0.6	10.2	1.6
Lo (3.4–7.0 m)	5.6	9.3	0.9	5.4	2.2
Radotín *Sc* (0.0–1.15 m)	6.9	10.4	0.7	7.4	2.5
Lo (1.2–3.45 m)	5.9	6.5	0.6	3.8	1.9
Podolí *Po* (0.0–1.65 m)	29.5	–	–	–	–
Sc (1.7–3.75 m)	3.3	16.1	0.7	12.7	2.5

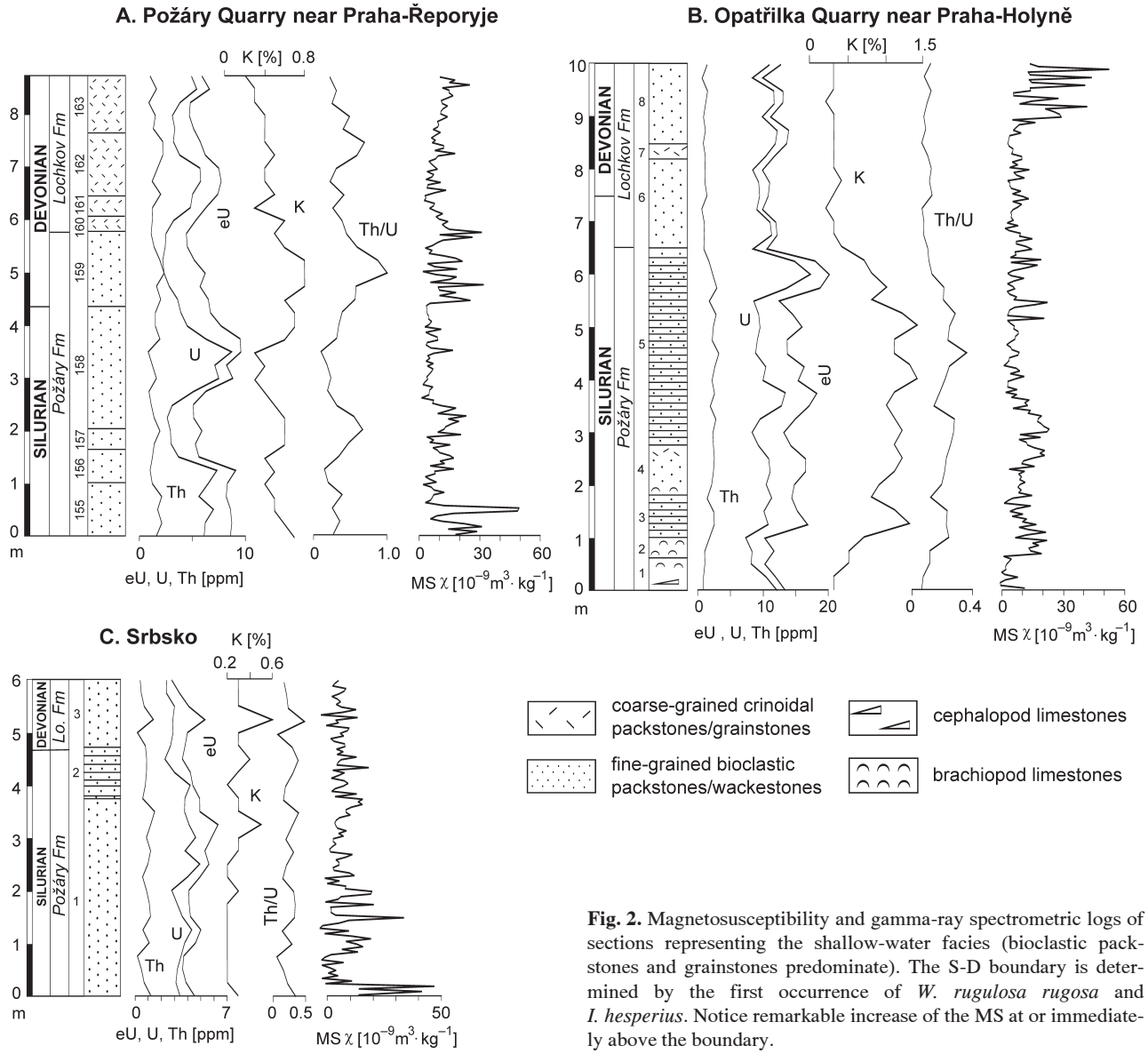

Fig. 2. Magnetosusceptibility and gamma-ray spectrometric logs of sections representing the shallow-water facies (bioclastic packstones and grainstones predominate). The S-D boundary is determined by the first occurrence of *W. rugulosa rugosa* and *I. hesperius*. Notice remarkable increase of the MS at or immediately above the boundary.

for Th) and shows only slight variations. The eU curves of all sections possess more or less conspicuous wave-like cyclic patterns.

Main characteristics of the MS and GRS records of the deep facies

Three different segments can be distinguished in the deep-water sections (mudstones/wackestones alternating with calcareous shales). The first one corresponds to the uppermost part of the Požáry Formation. It is characterized by high oscillations and the highest MS mean values in the studied sections (28.9–30.2 10^{-9} SI Units, maximum up to 95; Table 2). The overlying coarse-grained crinoidal limestones of the *Scyphocrinites* H (the lowermost part of the Lochkov Formation) have much lower average magnitudes (1.1–7.6 10^{-9} SI Units; see Fig. 3B–E). Amplitudes of the MS curves are also much lower. The upper segment corresponds to recovery of distal calciturbidite deposition higher in the sections. It is characterized by a slight increase in the MS (mean 5.6–10.2 10^{-9} SI Units), but not as high as in the uppermost part of the Požáry Formation.

The broader S-D interval is characterized by a remarkable decrease of the MS magnitudes associated with facies change (Fig. 3).

This facies shows much higher variations in the K content. The K concentrations are highest in the distal calciturbidite facies of the uppermost part of the Požáry Formation (average concentrations 1.7–1.9 %; Table 1). The K contents tend to decrease upwards and reach their minima within the *Scyphocrinites* H (average contents 0.5–0.7 %). The recovery of platy limestone/shale deposition is marked again by a slight increase in K concentrations (Fig. 3B–E). Generally, the amount of K shows excellent covariance with Th (R^2=0.87–0.98), while correlation between K and U and Th and U remains weak or has even slightly negative values (U topolů, Radotín,

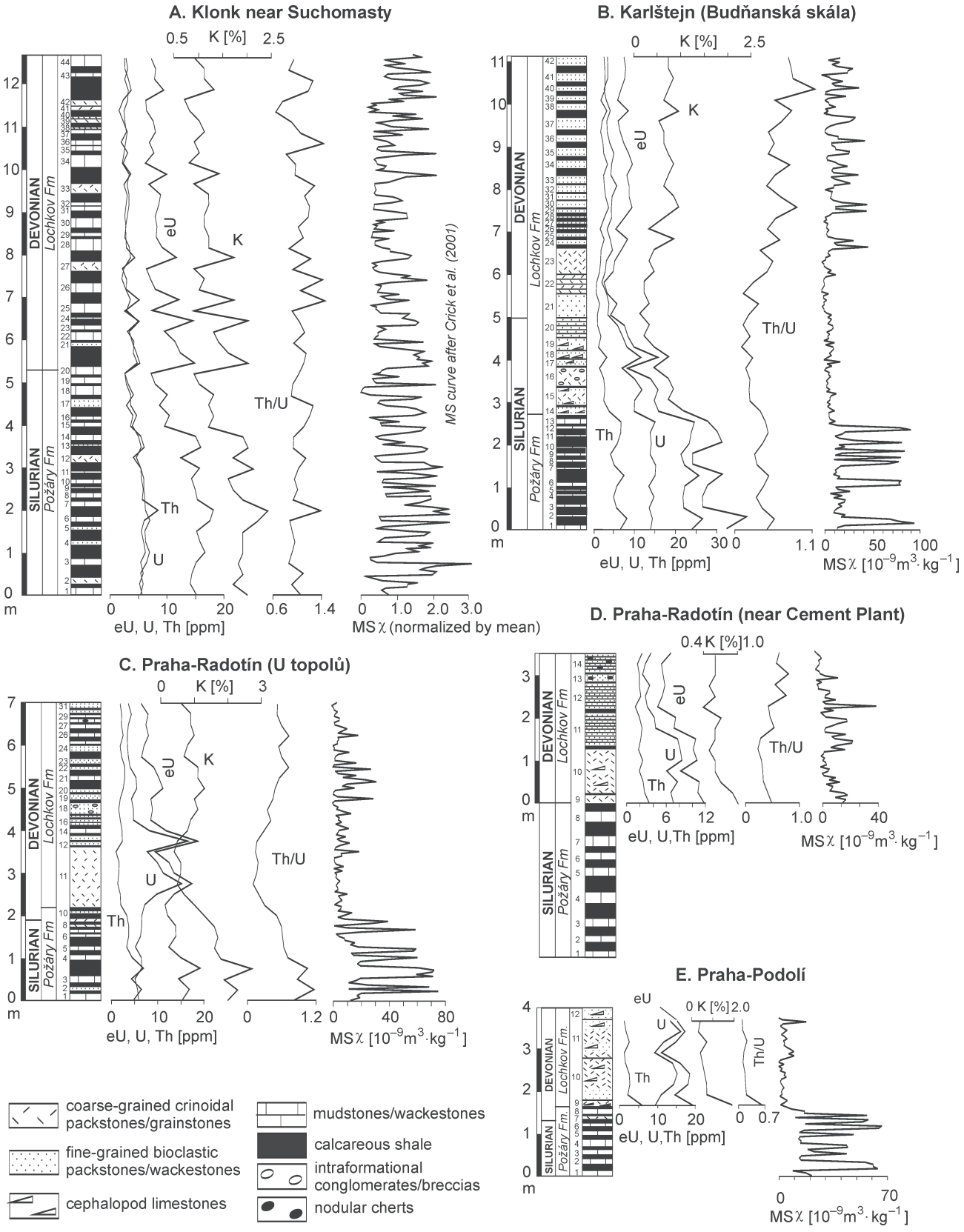

Fig. 3. Magnetosusceptibility and gamma-ray spectrometric record of sections representing the deep-water facies (slope distal calciturbidites predominate). The S-D boundary is determined by the first occurrence of *M. uniformis*. The lithological log of the GSSP at Klonk was modified after Chlupáč et al. (1972). The normalized MS curve was adopted from Crick et al. (2001).

and Podolí sections). Exceptionally, the Klonk and Karlštejn sections are characterized by good correlation between U and Th+K concentrations ($R^2 > 0.8$). This is expressed in similar trends and variations of K, U, Th and total gamma activity curves (see Fig. 3A and B). In the above mentioned three sections (U topolů, Radotín, Podolí), the eU variation is related mostly to changing U content (Fig. 3C–E).

The Th/U ratio is slightly higher than in the lower subtidal deposits, but only exceptionally exceeds 1 (average 0.21–1.02). In some sections this ratio tends to increase upwards (Karlštejn, Praha-Radotín sections, Fig. 3B–D).

The MS and GRS correlations of the studied sections

A crucial attempt to understand the high-resolution MS and GRS stratigraphy in the studied area is based on formalizing the MS and GRS patterns and their successions. Here, from technical viewpoint, it must be repeatedly stressed that all these MS sections were characterized using the 5 cm sampling but variable stratigraphic thicknesses were involved due to geological and geographical conditions. The "raw" MS data are plotted in Figs. 2 and 3, with exception of the GSSP Klonk section (Fig. 3A), which was adopted from the paper by Crick et al. (2001). The latter authors published the MS values normalized by their mean, so that the shape and patterns of the curve are not changed. This section is considered to be the standard for proposed stratigraphic correlations (see below).

In sections with similar facies development, several correlative MS patterns and their successions can be distinguished. The boundaries of these segments are mostly placed at local minima. These patterns are numbered by Roman numbers I, II, III, etc. Each pattern is characterized by a trend, magnitudes and amplitudes of the MS curve and number of main peaks. Each MS pattern usually contains several limestone beds (designated 1, 2, etc.) and shale interbeds (designated 1/2, etc.). Twelve patterns can be recognized in the deeper-water facies, while only 7 patterns are distinguished in the shallow-water (see Figs. 4 and 5). However, preliminary comparison of our sections showed that there are probably numerous stratigraphic gaps in the Praha-Podolí and Praha-Radotín sections (near the Cement plant). This assumption was also supported by biostratigraphic data (Chlupáč et al. 1972; Brocke et al. 2002; L. Slavík — pers. comm. 2007). Thus, we excluded these two sections from our further correlations as they might make our work rather speculative.

In spite of the scarcity of biostratigraphic indicators in some sections, they can be used at least for approximate control of the proposed more detailed MS-GRS correlations. As presented on Figs. 6 and 7, the MS record appears to be suitable tool for comparison of sections with roughly similar lithologies, namely 1) shallow-water bioclastic packstones/grainstones, and 2) deep-water distal calciturbidite mudstones/wackestones. However, the detailed correlation between these two contrasting facies is not fully clear. It is especially due to the sharp facies transition between carbonate lobes in proximal environments and flat calciturbidite fans in distal areas (Vacek 2007), but the possibility of eo-Variscan and younger tectonic obliteration of appropriate "transitional" facies developments must also be considered (Melichar & Hladil 1999; Melichar 2004 vs. Röhlich 2007).

As visible in Figs. 4 and 5, the thicknesses of distinguished patterns vary from section to section. This can indicate a fluctuation of depositional rates at the studied localities and/or insertion of erosional hiatuses. The partial erosion of older sediments was documented in both the relatively shallow- and deep-water conditions by eroded hardgrounds, erosional bases of distal calciturbidite beds or their common amalgamation (Vacek 2007).

The MS records can particularly be used for the more precise correlation between two standard sections, Klonk (Fig. 3A) and Karlštejn (Fig. 3B), which lithologically differ in the critical boundary interval. The boundary strata at Klonk are developed as platy mudstone/wackestone and calcareous shale interbeds, while at Karlštejn it consists of massive coarse-grained crinoidal and cephalopod packstones/grainstones with a bed of flat-pebble limestone conglomerates. In both sections, the S-D boundary is indicated by the first occurrence of the index graptolite *M. uniformis* (in the upper part of bed No. 20 at Klonk and in thin shale interbed No. 19/20 at Karlštejn, cf. Chlupáč et al. 1972). Using the MS curves, the S-D boundary at Klonk corresponds to the level within pattern *V*, which is characterized by solitary peaks at the base and the top and a group of several peaks in between. The boundary is located in the lower part of this pattern with increasing magnitudes (see Figs. 3A and 7). The same pattern (although with lower MS magnitudes) and level indicating the S-D boundary can be traced in the Karlštejn sequence (Figs. 3B and 7), but approximately 0.5 m below the first appearance of *M. uniformis*. Thus, we have to consider a diachronous first occurrence (or preservation) of this index species at Karlštejn and take it into account in local biostratigraphy of this area.

The combination of the MS and GRS (eU) data certainly decreases the risk of miscorrelation in this mosaic of facies (Figs. 6 and 7). The GRS curves also possess several features, which can be recognized in most of the sections and approximately fit the above suggested MS correlation of the studied sections. Here, it must be emphasized again that it also has at least approximate biostratigraphic control.

It is remarkable that even the uppermost Silurian part of the Klonk section is characterized by upwards decreasing of the eU values, which is followed by a distinctive peak (related to enhanced concentrations of K, U, and Th) just above the S-D boundary. This peak is clearly recognized in the other sections (e.g. Karlštejn, U topolů; Fig. 7), where it should indicate precisely the correlative point for the S-D boundary. However, this is not in agreement with the biostratigraphically determined boundaries and could signify a diachronous onset of index fossils over the region; either it is the case of their real occurrences, or it is a consequence of the always limited depth of sampling and investigation. For example, the comparison of two standard sections shows that GRS-based S-D boundary at Karlštejn is approximately 0.6 m lower than the first occurrence of *M. uniformis*, and this also fits well with the MS correlation of these stratotypes (see above; Fig. 7). Actually, it is not astonishing because we have to take into account the low preservation potential of pelagic

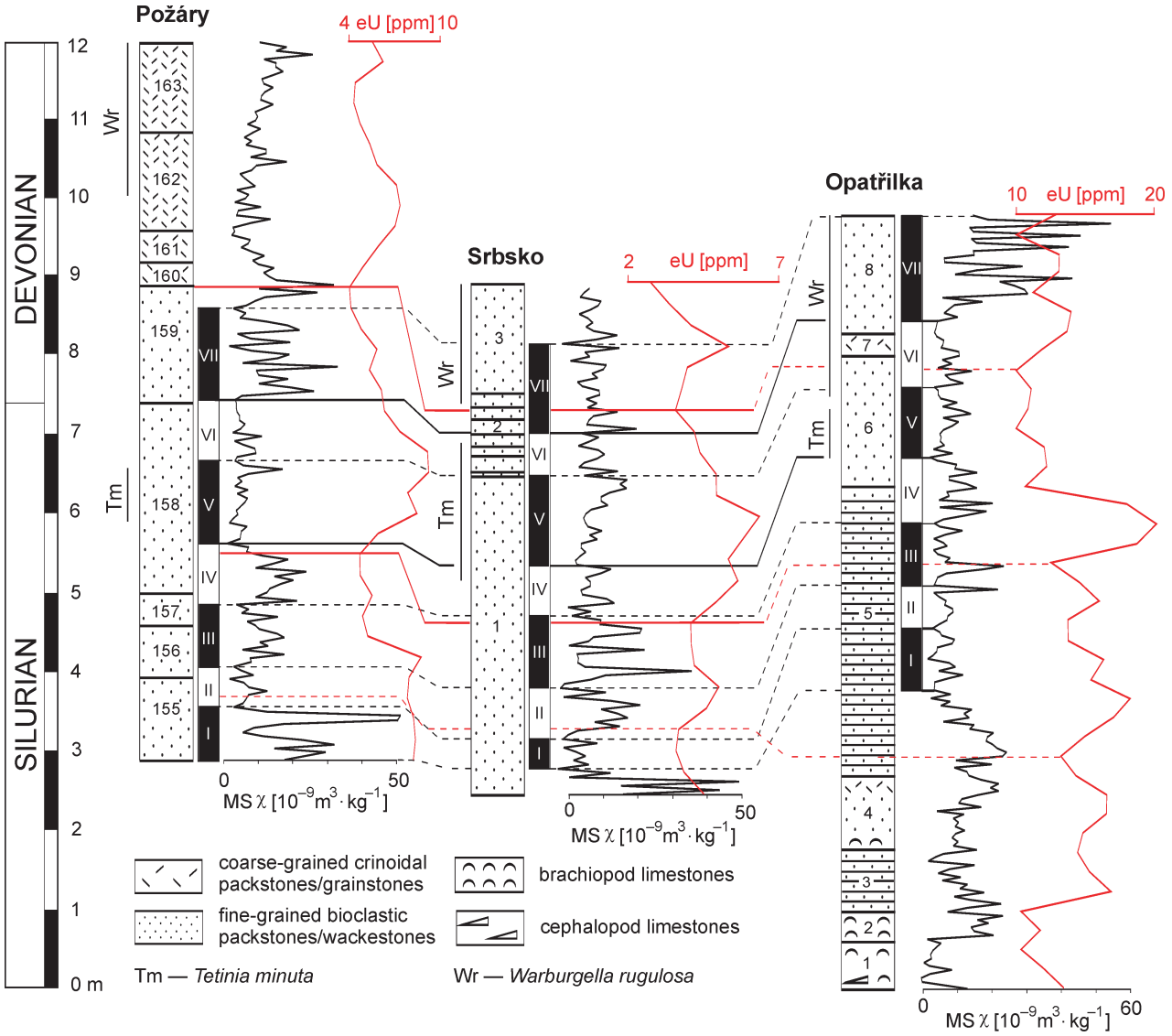

Fig. 4. The MS (**black lines**) and GRS (**red lines**) correlation of shallow-water sections. Correlative MS patterns are assigned by Roman numbers I–VII. Solid lines mark reliable, dashed lines mark less certain correlations. Taxon ranges after Chlupáč et al. (1972): solid lines indicate occurrence in this interval.

fossils in coarse-grained calciturbidites and mass flow conglomerates.

Magnetic susceptibility and mineral carriers

Several samples were collected from the studied sections for assessment of the magnetic composition of insoluble residue. These samples were taken in order to represent the main lithological types (macrofacies): crinoidal grainstones (Opatřilka Quarry, the upper part of bed No. 8; sample O8), coarse-grained crinoidal packstones of the *Scyphocrinites* H (Radotín — near the Cement Plant, the lower part of bed No. 10; sample R10), fine-grained mudstone to bioclastic wackestone (Karlštejn, bed No. 10; sample K10), laminated bioclastic wackestone (Karlštejn, bed No. 27), and calcareous shale (Karlštejn, bed No. 31/32). They were dissolved in 10% hydrochloric and acetic acids, separately. The amount of insoluble residue varies between 2 % (bioclastic packstones/grainstones) and 30 % (calcareous shales). The insoluble residues were analysed by X-ray diffraction (XRD), which identified common minerals including quartz (semi-quantitative content 60–80 %), albite (1–12 %), microcline (3–7 %), kaolinite (~1%), muscovite (5–10 %), chlorite-serpentine (1–12 %), and pyrite (1–20 %). However, some important magnetic minerals such as iron oxides may be leached during dissolution in acids. Therefore several rock magnetic methods applied to the whole-rock samples have been used for identification of them.

The results of rock magnetic analyses showed that most of the studied samples contain small amount of hematite, magnetite, and goethite. Our measured $B_{1/2}$ values for magnetite are in the range of 37–60 mT, hematite 63–200 mT, and goethite 1023–2884 mT. However, these minerals contribute only very little to the total MS (see Figs. 4 and 5). Both magnetite and

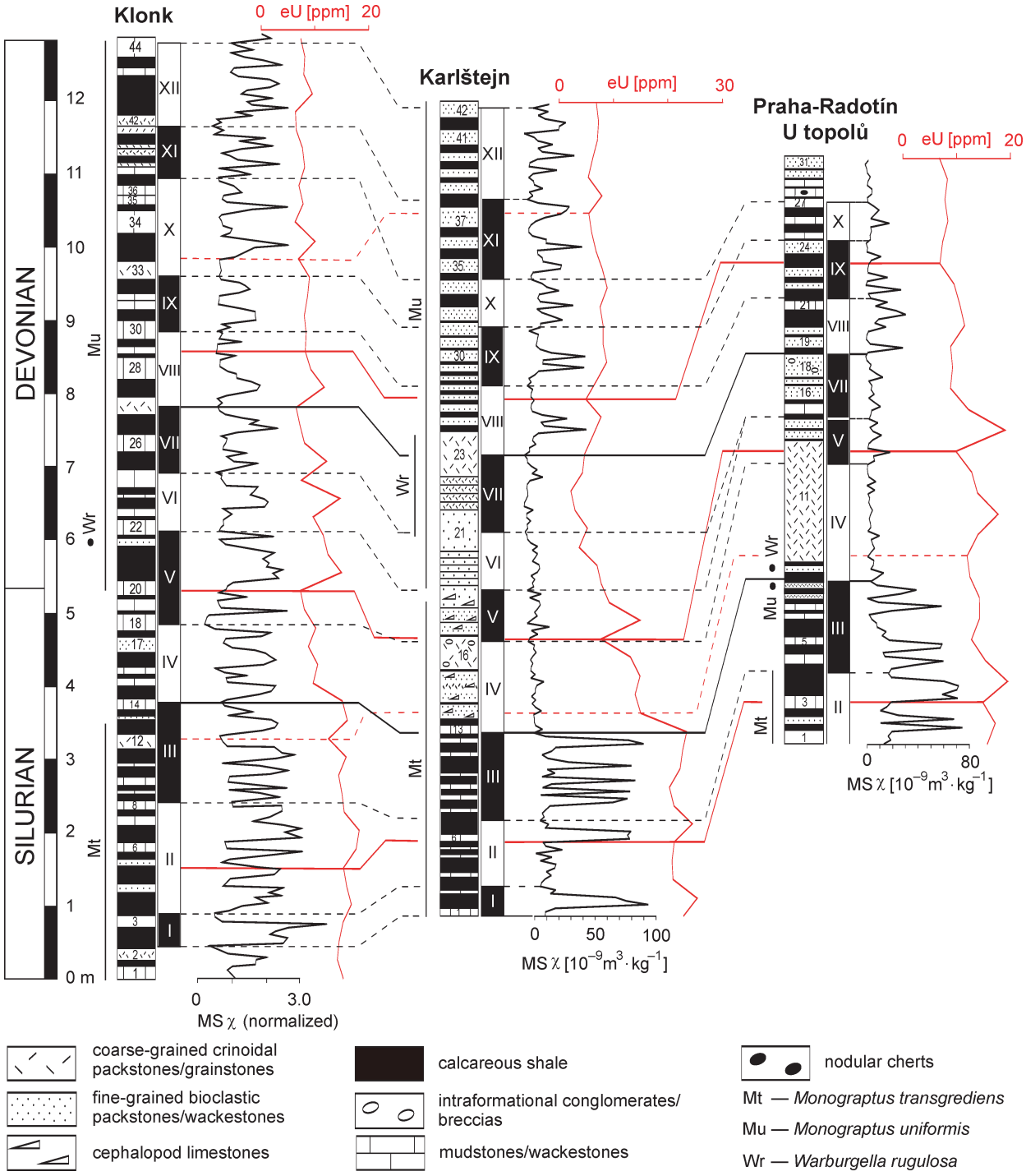

Fig. 5. The MS (**black lines**) and GRS (**red lines**) correlation of deep-water sections. Correlative MS patterns are assigned by Roman numbers I–XII. Solid lines mark reliable, dashed lines mark less certain correlation. Notice variable thickness or lack of distinguished MS patterns. It indicates unequal rate of preserved sediments due to variable supply or post-sedimentary erosion. Taxon ranges after Chlupáč et al. (1972) and Čáp et al. (2003): solid lines indicate occurrence in this interval, dots indicate occurrence in this bed only.

hematite can also be of diagenetic origin, while goethite is often a weathering product. If so its amount could not be related to depositional processes.

Possible effects of secondary magnetite and other ferromagnetic minerals have been tested by the IRM component analysis. Contribution of the above mentioned minerals has been measured on 37 samples with remarkably high or low MS. The percentage contribution of magnetite to the remanent magnetization has been compared with the bulk MS of the samples (Fig. 5). Their covariance is very low (R^2 = –0.34), showing that the MS does not depend on magnetite content, and thus the role of diagenetic magnetite may be excluded.

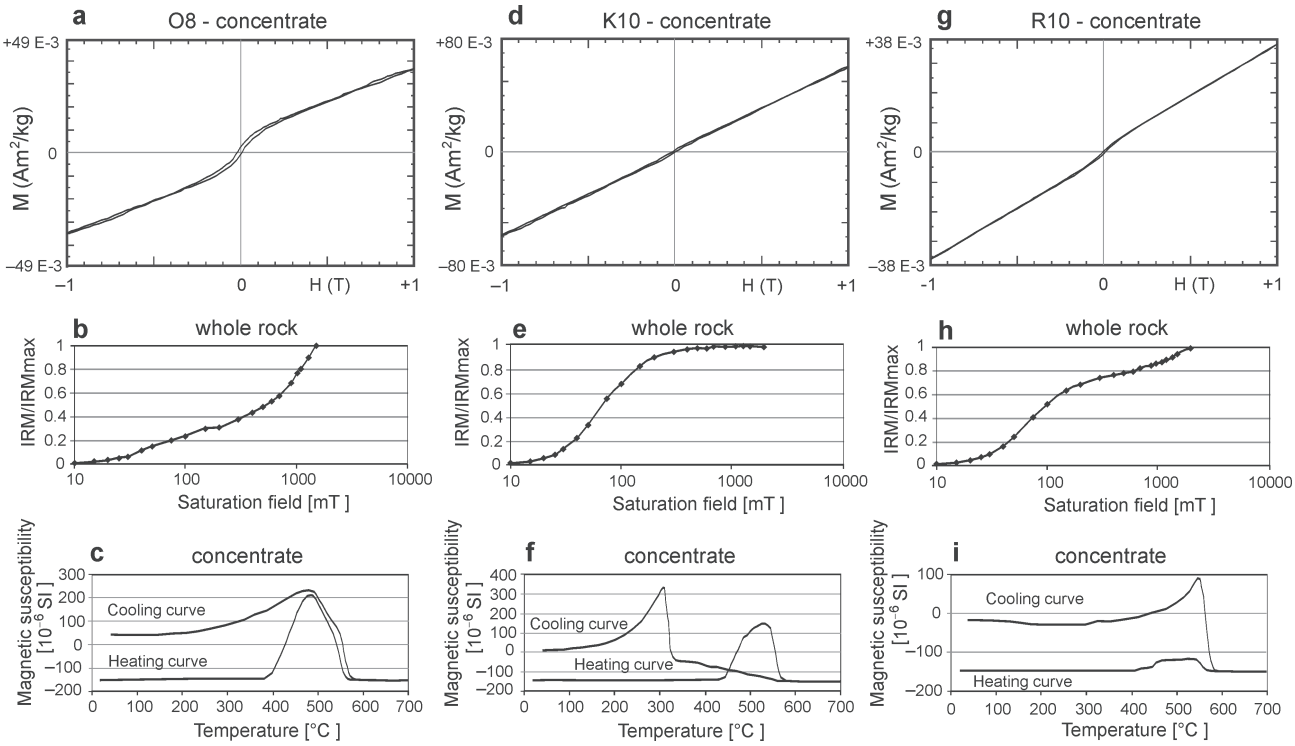

Fig. 6. Thermomagnetic and hysteresis behaviour of three mineral concentrates obtained by dissolution in acetic acid and isothermal remanent magnetization (IRM) curves measured on whole-rock samples. **Sample O8** (for description see the text): The hysteresis curve **a)** shows both paramagnetic and ferromagnetic behaviour. It is confirmed by the IRM acquisition curve **b)** with $B_{1/2}$ = 1071 mT typical for highly coercive goethite. The temperature variations of magnetic susceptibility **c)** indicate formation of magnetite between 400 and 500 °C. The Curie point of this magnetite is at 560 °C. **Sample K10**: The hysteresis curve **d)** indicates only paramagnetic behaviour. Nevertheless, the IRM acquisition **e)** proves that a small amount of low to medium coercivity mineral such as magnetite or hematite is present ($B_{1/2}$ = 72 mT). The temperature variations of susceptibility **f)** show formation of magnetite between the temperatures of 450 and 500 °C. The Curie point of this magnetite is at 570 °C. During progressive heating pyrrhotite is formed, its Curie is point at 320 °C. **Sample R10**: The hysteresis curve **g)** demonstrates paramagnetic behaviour and only subordinate indications of a ferromagnetic material. However, the IRM acquisition **h)** shows the presence of two different magnetic minerals: magnetite/hematite ($B_{1/2}$ = 70 mT) and goethite ($B_{1/2}$ = 2041 mT). The increase in magnetic susceptibility during heating above 400 °C **i)** is caused by newly-formed magnetite with the Curie point at 560 °C. Consequent heating creates pure magnetite with its Curie point at 580 °C.

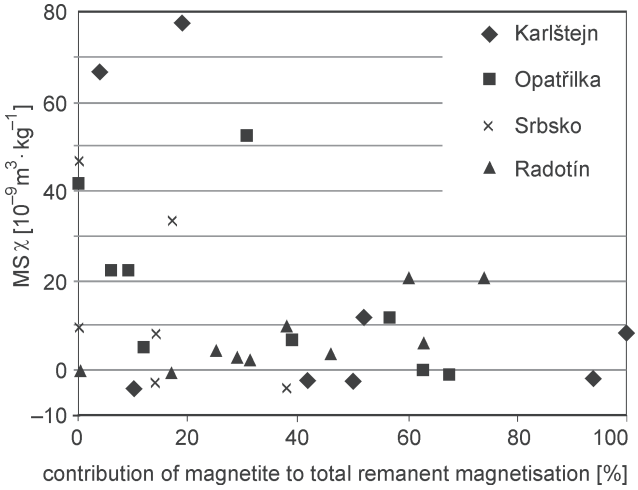

Fig. 7. Plot showing relationship between percentage magnetite contribution to the total remanent magnetization (IRM component analysis) and the MSχ. It is obviously weak (R^2 = –0.34) so that we can exclude possible effect of secondary diagenetic magnetite on the MS variations.

The major effects on rock magnetic susceptibility must be ascribed to varying amounts of paramagnetic detrital minerals (e.g. iron-bearing muscovite, chlorite) and only subordinately to oxides and sulphides (hematite/maghemite, pyrite/pyrrhotite). This fact justifies our following interpretations of the MS stratigraphic variations with respect to changing input of eroded detrital material related to sea-level fluctuations.

It is surprising that illite, which was often reported as an abundant component of the insoluble residues in the Požáry Formation on many places of the Prague Synclinorium (Suchý & Rozkošný 1996; Suchý et al. 1996) was not found. On the other hand, the indicated amounts of white mica are considerably higher than normally expected. It also belies the infrared-absorption and chemically based detections of up to several per cent of illite in the S-D sediments at Klonk (Hladil 1992) where the XRD evidence was also unclear. In this case, it was tentatively explained that due to the extensive damage to illite structures in ultrafine subcrystalline mixtures with quartz, organic matter, and carbonates. The absence of typical illite spectra in XRD diagrams can be explained by its low relative concentrations at ~1 % or less, but the possible presence

of both very high and very low crystalline forms related to illite remains unsolved.

The greatly increased amounts of albite and microcline are interesting in comparison with the proportions of plagioclases, pyroxenes and amphiboles, which were detected in these rocks together with small, basalt related volcaniclastic grains by direct observation and Energy Dispersive X-ray Spectroscopy (EDX; e.g. Hladil 1992), but which have no significant record in XRD. At least some of these albites and microclines can be considered authigenic, but the differentiation between the detrital and authigenic populations according to their crystal shapes and compositions (cf. Kastner 1971; Kastner & Siever 1979; Mišík 1994) does not yet provide unambiguous evidence in favour of this origin. Of course, quartz and also kaolinite (to lesser extent) are probably not only of purely detrital origin (Hladil 1992).

Interpretation of the MS and GRS records

The MS and GRS variations can be used not only for stratigraphic correlations of the studied sections but also for interpretation of sedimentary environments and their evolution (especially in combination with sedimentological data). It is based on methods and principles described in chapter Methods.

The lowermost Lochkovian (and approximately the basal part of the Lochkov Formation) in the shallow-water sections is characterized by an abrupt increase of the MS (Fig. 2). On the other hand, the eU curves mostly exhibit decreasing trend in the proximity of the S-D boundary (Fig. 2). It is mostly related to decline of U content. It does not need to respond to the decreasing content of clay, however. Very low covariance of K and U contents indicates different natures and sources of these two components. Potassium is related to clay minerals and K-feldspar, while U is also known to be significantly trapped in organic matter. A slight increase of K concentrations immediately above this pattern is indicative of higher amount of clay minerals.

Thus, both magnitudes indicate enhanced amount of non-carbonate impurities (magnetic components and clay) and may be interpreted as a result of sea-level fall, which caused increased erosion and terrigenous influx to marine environments (Ellwood et al. 2000). This is in accordance with sedimentological data, which also suggest a shallowing trend in the lowest parts of the Lochkov Formation (approximately the base of Lochkovian). It is expressed in partial sorting and reworking/rounding of bioclasts and washing out of fine-grained matrix in grainstone deposits in contrast to underlying strata (Vacek 2007).

In deep-water facies the high oscillation of the MS curve in the upper part of the Požáry Formation (generally the uppermost Pridoli) is related to alternation of limestone and shale interbeds (Figs. 3 and 8). It is noticeable that there are a number of analysed limestone beds, which have higher MS values than the background hemipelagic shale interbeds, which usually possess a higher amount of insoluble residue. It may be indicative of larger amount of detrital magnetic particles delivered to the basin with calciturbidites. The short-term facies change occurring in the slope environment as the *Scyphocrinites* H at the base of the Lochkov Formation (and close to the S-D boundary) is usually interpreted as a result of a relative sea-level fall, which caused increased erosion in shallow-water areas (e.g. Kříž et al. 1986; Chlupáč & Kukal 1988; Crick et al. 2001; Vacek 2007). Such facies changes indicating relative shallowing of sedimentary environments have been described from other regions of Europe (e.g. Carnic Alps — Schönlaub et al. 1994), and North America (e.g. central Nevada — Klapper & Murphy 1975; Matti & McKee 1977; Appalachian Basin — Denkler & Harris 1988). However, this event should be accompanied by increased magnitudes of the MS with enhanced supply with terrigenous detrital magnetic particles. It is interesting that the MS of these rocks is much lower than of the underlying limestone/shale sequence (Fig. 3). It might be explainable either by dispersion of fine-grained magnetic particles in the bulk of calcium carbonate (carbonate dilution effect) or by significant washing-out before re-deposition to slope and toe-of-slope environments (e.g. da Silva & Boulvain 2006). More properly, the observed effects of irregular washing of fine-grained matrix (often combined with current-driven orientation of cephalopod shells in these beds) suggest condensed deposition affected by bottom currents. Another explanation of deposition of *Scyphocrinites* H occurring in the described facies mosaics may be increased local subsidence at synsedimentary growth faults (namely "the precursor" Koda Fault, as presumed e.g. by Kříž 1992 or Vacek 2007) and a large amount of carbonate material with primary low concentrations of magnetic minerals derived from the upper part of the slope (as documented by the presence of carbonate lithoclasts derived from slope areas). Thus, this locally developed rapid carbonate sedimentation alternating with periods of sedimentary starvation is not expressed in enhanced MS values. Another explanation of the decline of the MS can be proposed as a restriction of terrigenous input during transgression. According to Schlager et al. (1994), the maximum thickness of calciturbidites corresponds to periods of increased carbonate production during sea-level rise (highstand shedding).

An evident decreasing eU tendency from the upper Požáry Formation to the lowermost Lochkov Formation (related to concurrently decreasing K, U, and Th concentrations) was documented in records from the deep-water sections (especially Klonk and Karlštejn; Fig. 3). In the latter, it culminates within the *Scyphocrinites* H. The overlying limestone/shale sequence of the Lochkov Formation is again characterized by a slight increase of detected GRS values (Fig. 3). Here, the main eU peaks partly correspond to background shale sediments with greater proportion of insoluble residue (namely clay minerals). However, there are also peaks situated within the seemingly massive bedding sets of proximal, often amalgamated calciturbidites (Karlštejn or Radotín-U topolů; Fig. 3B and C). At the U topolů section two distinctive U peaks (related to the GRS-based concentrations of 15.1 and 16.4 ppm) are situated within and slightly above the *Scyphocrinites* H (bed 11, section 2.75 and 3.75 m — Fig. 3C), which do not match enhanced K and Th values. Uranium is known to be highly mobile during diagenesis, so these enormous peaks may correspond to post-sedimentary concentration or indicate consider-

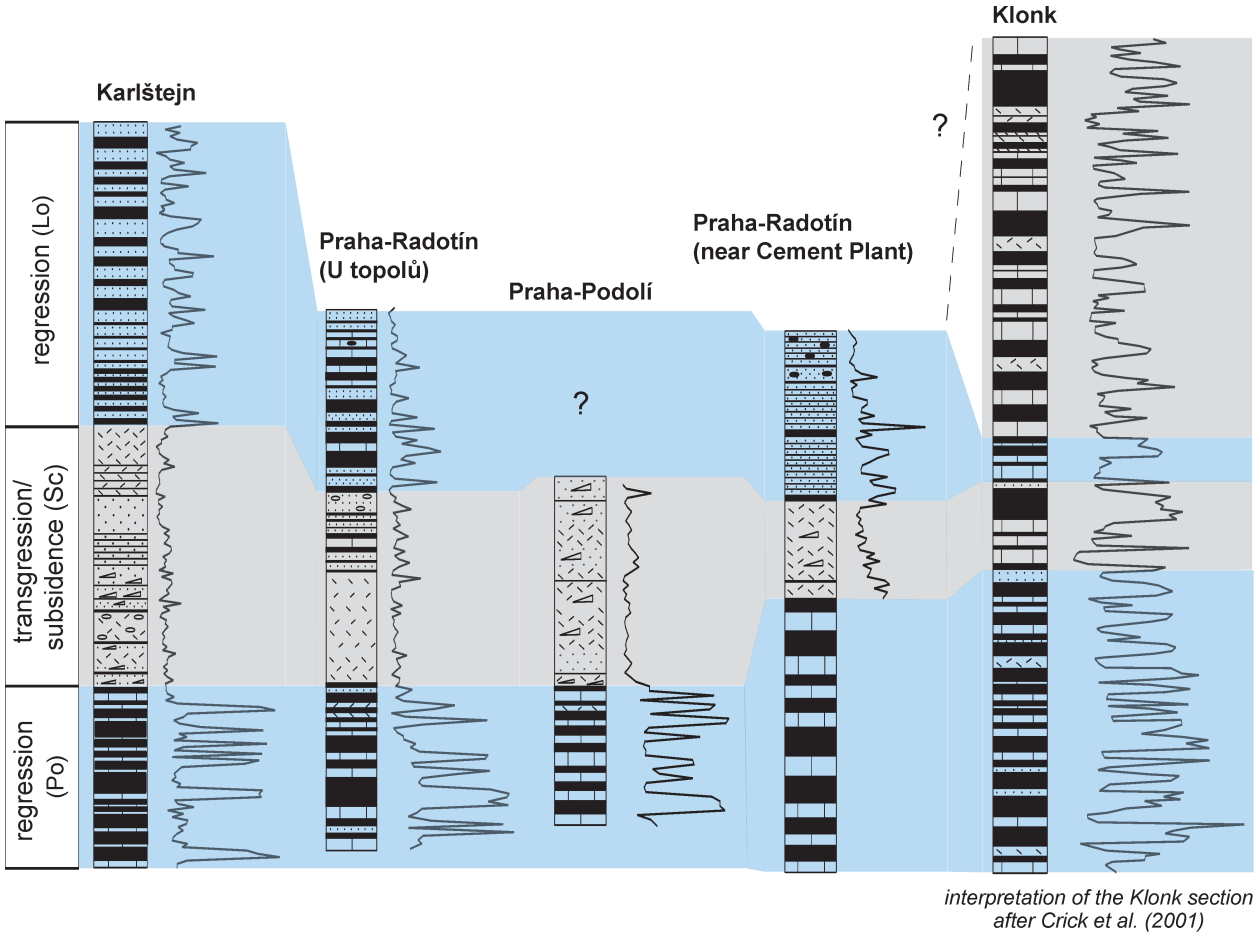

Fig. 8. Interpretation of the sea-level changes based on the MS records of the deep-water sections. Interpretation of the Klonk section was adopted from Crick et al. (2001), our results correspond in its lower part, but differs in the upper. **Po** — the upper part of the Požáry Fm, **Sc** — *Scyphocrinites* H., **Lo** — the lower part of the Lochkov Fm.

able dissolution (in some beds stylolites or extensive dissolutions can be observed). However, similar peaks can be traced at least in two other sections (Klonk section 5.5 m and Karlštejn section 4.0 m; Fig. 3A and B) and may therefore correspond to some widespread basinal events such as hiatuses or periods of sedimentary starvation, or delivery and concentration of exotic U-rich material.

At least three models must be considered for prograding of basinal carbonate deposits with reduced shale intercalations: 1) the increased input of eroded material from shallow-marine areas during the falling stage and lowstand system tracts; 2) the opposite situation of a period of enhanced carbonate production during the transgressive pulse, accompanied by highstand shedding effect (Schlager et al. 1994), and 3) other environmental effects influencing the shallow-water carbonate factories or pelagic carbonate productivity would be employed (e.g. increased abundance of pelagic crinoids, cephalopods).

Our interpretation based on evaluation of the GRS and MS records of the slope facies and comparison with published data is as follows: the uppermost part of the Požáry Formation has a regressive character, which is expressed in high MS and eU values (Figs. 3 and 8). Decreased carbonate productivity and low depositional rates have been accompanied by lithification of the sea-bottom. The lowermost part of the Lochkov Formation reflects a transgressive pulse, which resulted in decreased input of terrigenous material and pronounced decline of both magnitudes (Figs. 3 and 8). It was followed by slight MS and eU rise, which responded to gradual regression. However, it is possible that deepening during the S-D interval was caused by local sea-bottom subsidence and delivery of lithified deposits from underlying strata. The following regression might have corresponded to a eustatic sea-level fall well documented in shallow-marine areas. The deposition of the *Scyphocrinites* H also did not have to result only from increased supply of eroded material, which was formerly accumulated on appropriate shallower-water parts of the slope but rather was related to the mass development of floating echinoderms in general, as their distribution is widespread across the area and in many regions worldwide. Although it is certainly less conspicuous in the shallow-water deposits composed mostly of crinoidal limestones, thicker accumulations of *Scyphocrinites* debris are known, for example in the Daleje Valley (between the Požáry Q and Opatřilka sections).

This interpretation is partly in agreement with Crick et al. (2001), who presumed pronounced regression during the late Pridoli followed by a moderate transgressive/regressive pulse

in the critical S-D interval. According to results of the last mentioned study, the earliest Lochkovian has a clearly transgressive trend (focused on Klonk), and this is in contrast to our present results, which are based on several juxtaposed sections. The locally protracted high MS values with slowly decreasing GRS values in the combination with the presence of coarse-grained crinoidal beds up to the lower Lochkovian (magnetic intervals *VII–VIII*) are unexpected or even counter-intuitive with the first lower Lochkovian transgressive episode (compare Fig. 8 herein to figs. 3, 4 in Crick et al. 2001).

However, we are aware that there are also alternative interpretations based on the MS and GRS variations and other data (e.g. carbon and oxygen isotopes) described in numerous papers from the Silurian and Devonian of the Prague Synclinorium and other regions. Due to limited space we briefly refer for discussion to Hladíková et al. (1997), Slavík et al. (2000), Mann et al. (2001), Saltzman (2002), Buggisch & Mann (2004), Buggisch & Joachimski (2006), Bábek et al. (2007), and Malkowski et al. (2009).

Conclusions

The combined MS-and-GRS stratigraphic assessment and regional comparison of the carbonate facies around the S-D boundary in the Prague Synclinorium showed a significantly good correlative value between sections with similar facies development (i.e. lower subtidal to upper slope bioclastic grainstones/packstones and lower slope to toe-of-the-slope calciturbidites with predominance of bioclastic and peloidal wackestones/mudstones and calcareous shales). This comparison shows that the onset of the index species and the biostratigraphically determined S-D boundary may be diachronous and highly depend on facies. This fact makes the MS-and-GRS stratigraphy a powerful tool for precise correlation within the region. It also proved remarkable condensation and gaps in sedimentary record, especially in the lower slope conditions where distal calciturbidites predominate.

A major effect on the MS is ascribed to paramagnetic minerals, which have been delivered to the basin from land. Therefore, we can relate the changing amount of this terrigenous material detected by the MS and GRS to fluctuating erosion and sea-level changes.

The critical S-D interval is characterized in relatively shallow marine areas by increased values of MS, which are interpreted as related to a higher influx of terrigenous material during a regressive pulse. This interpretation is supported by contemporaneous increasing concentrations of GRS-detected potassium (clay) and is also supported by sedimentological evidence.

On the contrary, a broader S-D interval in the deep-water facies is characterized by visible facies change and decreasing of the MS values. Maxima of MS and GRS in the uppermost part of the Požáry Formation (generally upper Pridoli) are interpreted as a response to a regressive phase associated with a low depositional rate and sea-bottom lithification. The very lowermost part of the Lochkov Formation (generally the base of the Lochkovian) reflects a transgressive pulse leading to decreased input of terrigenous material and distinctive decline of both magnitudes. The overlying sequence characterized by slightly rising MS and eU corresponds to gradual regression. The deepening trend during the S-D interval was probably accompanied by local subsidence and influx of eroded lithoclastic material. The following regression may reflect a eustatic sea-level drop well supported by evidence from the shallowest marine areas. The facies change close to the S-D boundary and deposition of the *Scyphocrinites* H might predominantly result from a biotic event unrelated to sea-level changes and local subsidence, rather than from sea-level rise/drop.

Acknowledgments: We are grateful to A.C. da Silva, F. Hrouda and one anonymous reviewer for valuable comments and suggestions, which helped improve the original manuscript. Special thanks are due to colleagues who provided the complementary analyses used for the interpretation (V. Goliáš, XRD, Charles University, Prague; A. Langrová, EDX, WDS; P. Pruner, Academy of Sciences, Prague, rock magnetism), and those who discussed environmental constraints (J.E. Barrick, Texas Tech University, Lubbock, M.A. Murphy, University of California, Riverside and L. Slavík , Academy of Sciences, Prague) and the importance of the Klonk MS section and observed periodicities (B.B. Ellwood, Louisiana State University, Baton Rouge). The role of framework grants is appreciated (MSM 0021620855, AV0Z30130516, IAA300130702, IGCP 580).

References

Bábek O., Přikryl T. & Hladil J. 2007: Progressive drowning of carbonate platform in the Moravo-Silesian Basin (Czech Republic) before the Frasnian/Famenian event: facies, compositional variations and gamma-ray spectrometry. *Facies* 53, 293–316.

Brocke R., Wilde V., Fatka O. & Mann U. 2002: Chitinozoa and acritarchs at the Silurian/Devonian boundary: Examples from the Barrandian area. In: Brock G.A. & Talent J. (Eds.): 1st International Palaeontological Congress. *Abstracts,* Sydney, 192.

Brocke R., Fatka O. & Wilde V. 2006: Acritarchs and prasynophytes of the Silurian-Devonian GSSP (Klonk, Barrandian area, Czech Republic). *Bull. Geosci.* 81, 1, 27–41.

Buggisch W. & Joachimski M.M. 2006: Carbon isotope stratigraphy of the Devonian of Central and Southern Europe. *Palaeogeogr. Palaeoclimatol. Palaeoecol.* 240, 68–88.

Buggisch W. & Mann U. 2004: Carbon isotope stratigraphy of Lochkovian to Eifelian limestones from the Devonian of central and southern Europe. *Int. J. Earth Sci.* 93, 521–541.

Carls P., Slavík L. & Valenzuela-Ríos J.I. 2007: Revisions of conodont biostratigraphy across the Silurian-Devonian boundary. *Bull. Geosci.* 82, 2, 145–164.

Chlupáč I. & Kukal Z. 1988: Possible global events and the stratigraphy of the Barrandian Paleozoic (Cambrian–Devonian, Czechoslovakia). *Sbor. Geol. Věd, Geol.* 43, 83–146.

Chlupáč I., Jaeger H. & Zikmundová J. 1972: The Silurian-Devonian boundary in the Barrandian. *Bull. Canad. Petrol. Geol.* 20, 104–174.

Chlupáč I., Havlíček V., Kříž J., Kukal Z. & Štorch P. 1998: Palaeozoic of the Barrandian (Cambrian to Devonian). *Czech Geol. Surv.*, Prague, 1–183.

Crick R.E., Ellwood B.B., El Hassani A., Feist R. & Hladil J. 1997: Magnetosusceptibility event and cyclostratigraphy (MSEC) of the Eifelian-Givetian GSSP and associated boundary sequences

in north Africa and Europe. *Episodes* 20, 3, 167–175.

Crick R.E., Ellwood B.B., El Hassani A. & Feist R. 2000: Proposed magnetostratigraphy susceptibility magnetostratotype for Eifelian–Givetian GSSP (Anti-Atlas, Morocco). *Episodes* 23, 2, 93–101.

Crick R.E., Ellwood B.B., Hladil J., El Hassani A., Hrouda F. & Chlupáč I. 2001: Magnetostratigraphy susceptibility of the Přídolian–Lochkovian (Silurian–Devonian) GSSP (Klonk, Czech Republic) and a coeval sequence in Anti-Atlas Morocco. *Palaeogeogr. Palaeoclimatol. Palaeoecol.* 167, 73–100.

Crick R.E., Ellwood B.B., Feist R., El Hassani A., Schindler E., Dreesen R., Over D.J. & Girard C. 2002: Magnetostratigraphy susceptibility of the Frasnian/Famennian boundary. *Palaeogeogr. Palaeoclimatol. Palaeoecol.* 181, 67–90.

Čáp P., Vacek F. & Vorel T. 2003: Microfacies analysis of Silurian and Devonian type sections (Barrandian, Czech Republic). *Czech Geol. Surv., Spec. Pap.* 15, 1–40.

da Silva A.C. & Boulvain F. 2006: Upper Devonian carbonate platform correlations and sea level variations recorded in magnetic susceptibility. *Palaeogeogr. Palaeoclimatol. Palaeoecol.* 240, 373–388.

da Silva A.C., Mabille C. & Boulvain F. 2009a: Influence of sedimentary setting on the use of magnetic susceptibility: examples from Devonian of Belgium. *Sedimentology* 56, 1292–1306.

da Silva A.C., Potma K., Weissenberger J.A.W., Whalen M.T., Mabille C. & Boulvain F. 2009b: Magnetic susceptibility evolution and sedimentary environments on carbonate platform sediments and atolls, comparison of the Frasnian from Belgium and from Alberta. *Sed. Geol.* 214, 3–18.

da Silva A.C., Yans J. & Boulvain F. 2010: Early–Middle Frasnian (early Late Devonian) sedimentology and magnetic susceptibility of the Ardennes area (Belgium): identification of severe and rapid sea-level fluctuations. *Geologica Belgica* 13, 4, 319–332.

Denkler K.E. & Harris A.G. 1988: Conodont-based determination of the Silurian-Devonian boundary in the Valley and Ridge Province, Northern and Central Appalachians. *US Geol. Surv. Bull.* B 1837, B1–B13.

Durrance E.M. 1986: Radioactivity in geology: principles and applications. *Ellis Horwood*, Chichester, 1–441.

Ellwood B.B., Chrzanowski T.H., Hrouda F., Long G.J. & Buhl M.L. 1988: Siderite formation in anoxic deep-sea sediments: a synergetic bacterially controlled process with important implications in paleomagnetism. *Geology* 16, 980–982.

Ellwood B.B., Crick R.E., El Hassani A., Benoist S.L. & Young R.H. 2000: Magnetosusceptibility event and cyclostratigraphy method applied to marine rocks: Detrital input versus carbonate productivity. *Geology* 28, 12, 1135–1138.

Ellwood B.B., Crick R.E., Garcia-Alcade Fernandez J.L., Soto F.M., Truyóls-Massoni M., El Hassani A. & Kovas E.J. 2001: Global correlation using magnetic susceptibility data from Lower Devonian rocks. *Geology* 29, 7, 583–586.

Ellwood B.B., Garcia-Alcade Fernandez J.L., El Hassani A., Hladil J., Soto F., Truyóls-Massoni M., Wedigge K. & Koptíková L. 2006: Stratigraphy of the Middle Devonian boundary: Formal definition of the susceptibility magnetostratotype in Germany with comparisons to sections in the Czech Republic, Morocco and Spain. *Tectonophysics* 418, 31–49.

Fiala F. 1970: Silurian and Devonian diabases of the Barrandian. *Sbor. Geol. Věd, Geol.* 17, 7–97 (in Czech).

Frederichs T., Dobeneck T. Von, Bleil U. & Dekkers M.J. 2003: Towards the identification of siderite, rhodochrosite, and vivianite in sediments by their low-temperature magnetic properties. *Phys. Chem. Earth* 28, 669–679.

Frýda J., Hladil J. & Vokurka K. 2002: Seawater strontium isotope curve at the Silurian/Devonian boundary: a study of the global Silurian/Devonian boundary stratotype. *Geobios* 35, 21–28.

Geršl M. & Hladil J. 2004: Gamma-ray and magnetic susceptibility correlation across a Frasnian carbonate platform and the search for "punctata" equivalents in stromatoporoid-coral limestone facies of Moravia. *Geol. Quart.* 48, 3, 283–292.

Grygar T., Dědeček J., Kruiver P.P., Dekkers M.J., Bezdička P. & Schneeweiss O. 2003: Iron oxide mineralogy in late Miocene red beds from La Gloria, Spain: rock-magnetic, voltammetric and Vis spectroscopy analyses. *Catena* 53, 2, 115–132.

Herten U. 2000: Petrographische und geochemische Charakterisierung der Pelit-Lagen aus der Forschungsbohrung Klonk-1 (Suchomasty/Tschechische Republik). *Ber. Forschungszentrum Jülich* 3751, 1–78.

Hladil J. 1991: Evaluation of the sedimentary record in the Silurian/Devonian boundary stratotype at Klonk (Barrandian area, Czechoslovakia). *Newslett. Stratigr.* 25, 2, 115–125.

Hladil J. 1992: Are there turbidites in the Silurian/Devonian boundary stratotype (Klonk near Suchomasty, Barrandian, Czechoslovakia)? *Facies* 26, 35–54.

Hladil J. 2002: Geophysical records of dispersed weathering products on the Frasnian carbonate platform and early Famennian ramps in Moravia, Czech Republic: proxies for eustasy and palaeoclimate. *Palaeogeogr. Palaeoclimatol. Palaeoecol.* 181, 213–250.

Hladil J., Bosák P., Jansa L.F., Těžký A., Helesicová K., Hrubanová J., Pruner P., Krůta T., Špaček P. & Chadima M. 2000: Frasnian eustatic cycles viewed with gamma spectrometric and magneto-susceptibility stratigraphy tools (Moravia): Six major floodings on cratonized basement. *Subcommission on Devonian Stratigraphy, Newsletter* 17, 48–52.

Hladil J., Bosák P., Slavík L., Carew J.L., Mylroie J.E. & Geršl M. 2003a: A pragmatic test of early origin and fixation of gamma-ray spectrometric (U, Th) and magneto-susceptibility (Fe) patterns related to sedimentary cycle boundaries in pure platform limestones. *Carbonate Evaporite* 18, 2, 89–107.

Hladil J., Bosák P., Slavík L., Carew J.L., Mylroie J.E. & Geršl M. 2003b: Early diagenetic origin and persistence of gamma-ray and magnetosusceptibility patterns in platform carbonates: comparison of Devonian and Quaternary sections. *Phys. Chem. Earth* 28, 719–727.

Hladil J., Geršl M., Strnad L., Frána J., Langrová A. & Spišiak J. 2006: Stratigraphic variations of complex impurities in platform limestones and possible significance of atmospheric dust: a study with emphasis on gamma-ray spectrometry and magnetic susceptibility outcrop logging (Eifelian–Frasnian, Moravia, Czech Republic). *Int. J. Earth Sci.* 95, 4, 703–723.

Hladíková J., Hladil J. & Kříbek B. 1997: Carbon and oxygen isotope record across Pridoli to Givetian stage boundaries in the Barrandian basin (Czech Republic). *Palaeogeogr. Palaeoclimatol. Palaeoecol.* 132, 225–241.

Hrouda F. 1994: A technique for the measurement of thermal changes of magnetic susceptibility of weakly magnetic rocks by the CS-2 apparatus and the KLY-2 Kappabridge. *Geophys. J. Int.* 118, 604–612.

Jelínek V. & Pokorný J. 1997: Some new concepts in technology of transformer bridges for measuring susceptibility anisotropy of rocks. *Phys. Chem. Earth* 22, 179–181.

Jeppsson L. 1988: Conodont biostratigraphy of the Silurian boundary stratotype at Klonk, Czechoslovakia. *Geologica et Palaeont.* 22, 21–31.

Jeppsson L. 1989: Latest Silurian conodonts from Klonk, Czechoslovakia. *Geologica et Palaeont.* 23, 21–37.

Kastner M. 1971: Authigenic feldspars in carbonate rocks. *Amer. Mineralogist* 56, 1403–1442.

Kastner M. & Siever R. 1979: Low temperature feldspars in sedimentary rocks. *Amer. J. Sci.* 279, 453–479.

Klapper G. & Murphy M.A. 1975: Silurian–Lower Devonian Conodont Sequence in the Roberts Mountains Formation of Central Nevada. *Univ. California Publ., Geol. Sci.* 111, 1–62.

Koptíková L., Hladil J., Slavík L. & Frána J. 2007: The precise position and structure of the Basal Choteč Event: Lithological, MS-and-GRS and geochemical characterisation of the Emsian-Eifelian carbonate stratal successions in the Prague Syncline (Teplá-Barrandian Unit, Central Europe). In: Over D.J. & Morrow J. (Eds.): Subcommission on Devonian Stratigraphy and IGCP 499 Devonian Land Sea Interaction, Eureka NV 9-17 Sep 2007, Program and Abstracts. *Genesea*, NY, US, 55–57.

Koptíková L., Hladil J., Slavík L., Frána J. & Vacek F. 2008: Evidence of a significant change between Lochkovian and Pragian: detailed lithological, geophysical, geochemical and mineralogical aspects (Požáry 3 section in Prague Synform). In: El-Mehdawi A.D. & Koenigshof P. (Eds.): Abstracts of the Field Workshop IGCP 499 Devonian Land-Sea Interaction. *Libyan Petroleum Institute*, Tripoli, 10–14.

Koptíková L., Bábek O., Hladil J., Kalvoda J. & Slavík J. 2010: Stratigraphic significance and resolution of spectral reflectance logs in Lower Devonian carbonates of the Barrandian area, Czech Republic; a correlation with magnetic susceptibility and gamma-ray logs. *Sed. Geol.* doi: 10.1016/j.sedgeo.2010.01.004

Kranendonck O. 2000: Petrographische und geochemische Charakterisierung der Karbonatbänke aus der Forschungsbohrung Klonk-1 (Suchomasty/Tschechische Republik). *Ber. Forschungszentrum Jülich* 3750, 1–113.

Krs M. & Pruner P. 1995: Palaeomagnetism and palaeogeography of the Variscan formations of the Bohemian Massif, comparison with other European regions. *J. Czech Geol. Soc.* 40, 1–2, 3–46.

Krs M., Pruner P. & Man O. 2001: Tectonic and paleogeographic interpretation of the paleomagnetism of Variscan and pre-Variscan formations of the Bohemian Massif, with special reference to the Barrandian terrane. *Tectonophysics* 332, 93–114.

Kruiver P.P., Dekkers M.J. & Heslop D. 2001: Quantification of magnetic coercivity components by the analysis of acquisition curves of isothermal remanent magnetisation. *Earth Planet. Sci. Lett.* 189, 269–276.

Kříž J. 1992: Silurian field excursions. Prague Basin (Barrandian), Bohemia. *Nat. Mus. Wales, Geol. Ser.* 13, 1–111.

Kříž J., Jaeger H., Paris F. & Schönlaub H.P. 1986: Přídolí — the fourth subdivision of the Silurian. *Jb. Geol. Bundesanst.* 129, 2, 291–360.

Lis J., Pasieczna A., Strzelecki R., Wolkowicz S. & Lewandowski P. 1997: Geochemical and radioactivity mapping in Poland. *J. Geochem. Explor.* 60, 39–53.

Løvborg L., Wollenberg H., Sørensen P. & Hansen J. 1971: Field determination of uranium and thorium by gamma-ray spectrometry exemplified by measurements in the Ilimaussaq alkaline intrusion, South Greenland. *Econ. Geol.* 66, 368–384.

Malkowski K., Racki G., Drygant D. & Szaniawski H. 2009: Carbon isotope stratigraphy across the Silurian-Devonian transition in Podolia, Ukraine: evidence for a global geochemical perturbation. *Geol. Mag.* 146, 5, 674–689.

Mann U., Herten U., Kranendonck O., Poelchau H.S., Stroetmann J., Vos H., Wilkes H., Suchý V., Brocke R., Wilde V., Muller A., Ebert J., Bozdogan N., Soylu C., El Hassani A. & Yalcin M.N. 2001: Dynamics of the Silurian/Devonian boundary sequence: sedimentary cycles vs. organic matter variation. *Terra Nostra* 4, 44–48.

Matti J.C. & McKee E.H. 1977: Silurian and Lower Devonian paleogeography of the outer continental shelf of the Cordilleran Miogeocline, central Nevada. In: Stewart J.H., Stevens C.H. & Fritsche A.E. (Eds.): Paleozoic Paleogeography of the Western United States — Pacific Section. *SEPM*, Los Angeles, 181–215.

McLaren D.J. 1977: The Silurian-Devonian Committee. A final report. In: Martinsson A. (Ed.): The Silurian-Devonian boundary. *I.U.G.S. Ser. A* 5, 1–34.

Melichar R. 2004: Tectonics of the Prague Synform: a hundred years of scientific discussion. *Krystalinikum* 30, 167–187.

Melichar R. & Hladil J. 1999: Resurrection of the Barrandian nappe structures, central Bohemia. *Geolines* 8, 48–50.

Mišík M. 1994: Authigenic feldspars in carbonate rocks of the Western Carpathians. *Geol. Carpathica* 45, 103–111.

Paris F., Laufeld S. & Chlupáč I. 1981: Chitinozoa of the Silurian-Devonian boundary statotypes in Bohemia. *Sver. Geol. Unders., Ser. C* 4, 51, 1–29.

Parma J. & Zapletal K. 1991: CS-1 apparatus for measuring the temperature dependence of low-field susceptibility of minerals and rocks (in cooperation with the KLY-2 Kappabridge). *Leaflet, Geofyzika*, Brno.

Patočka F. & Štorch P. 2004: Evolution of geochemistry and depositional settings of Early Palaeozoic siliciclastics of the Barrandian (Teplá-Barrandian Unit, Bohemian Massif, Czech Republic). *Int. J. Earth Sci.* 93, 728–741.

Patočka F., Pruner P. & Štorch P. 2003: Palaeomagnetism and geochemistry of Early Palaeozoic rocks of the Barrandian (Teplá-Barrandian Unit, Bohemian Massif): palaeotectonic implications. *Phys. Chem. Earth* 28, 735–749.

Röhlich P. 2007: Structure of the Prague Basin: The deformation diversity and its causes (the Czech Republic). *Bull. Geosci.* 82, 2, 175–182.

Saltzman M.R. 2002: Carbon isotope ($\delta^{13}C$) stratigraphy across the Silurian-Devonian transition in North America: evidence for a perturbation of the global carbon cycle. *Palaeogeogr. Palaeoclimatol. Palaeoecol.* 187, 83–100.

SatisGeo, Ltd. 2009: GS-512 Gamma Ray Spectrometer. Manufacturer's leaflet with technical data. http://www.satisgeo.com/gs5.htm

Schlager W., Reijmer J.J.G. & Droxler A. 1994: Highstand shedding of carbonate platforms. *J. Sed. Res.* B64, 3, 270–281.

Schönlaub H.P., Kreuzer L., Joachimski M.M. & Buggisch W. 1994: Paleozoic boundary sections of the Carnic Alps (Southern Austria). *Erlanger Geol. Abh.* 122, 77–103.

Slavík L., Hladil J., Blažek R. & Krůta M. 2000: Anatomy of the Pragian stratigraphic column: gamma spectrometric record throughout complete 170-m thick Pragian section in calciturbidite/hemipelagite facies (Prague, section "Under Barrandov Bridge"). *Subcommission on Devonian Stratigraphy, Newsletter* 17, 46–47.

Suchý V. & Rozkošný I. 1996: Diagenesis of clay minerals and organic matter in the Pridoli Formation (Upper Silurian), the Barrandian Basin, Czech Republic: first systematic survey. *Acta Univ. Carol., Geol.* 38, 401–409.

Suchý V., Rozkošný I., Žák K. & Franců J. 1996: Epigenetic dolomitization of the Přídolí formation (Upper Silurian), the Barrandian basin, Czech Republic: implications for burial history of Lower Paleozoic strata. *Geol. Rundsch.* 85, 264–277.

Tauxe L., Mullender T.A.T. & Pick T. 1996: Pot-bellies, wasp-waists and superparamagnetism in magnetic hysteresis. *J. Geophys. Res.* 101, 571–584.

Vacek F. 2007: Carbonate microfacies and depositional environments of the Silurian-Devonian boundary strata in the Barrandian area (Czech Republic). *Geol. Carpathica* 58, 6, 497–510.